




Characterisation of hemidiaphragm dysfunction using dynamic chest radiography: a pilot study

Thomas Simon FitzMaurice^{1,2}, Caroline McCann³, Dilip S. Nazareth ^{1,4} and Martin J. Walshaw^{1,4}

¹Dept of Respiratory Medicine, Liverpool Heart and Chest Hospital, Liverpool, UK. ²Institute of Life Course and Medical Sciences, University of Liverpool, Liverpool, UK. ³Dept of Radiology, Liverpool Heart and Chest Hospital, Liverpool, UK. ⁴Institute of Infection and Global Health, University of Liverpool, Liverpool, UK.

Corresponding author: Thomas FitzMaurice (thomas.fitzmaurice@lhch.nhs.uk)



Shareable abstract (@ERSpublications)

[Dynamic chest radiography is a rapid, well-tolerated and straightforward chest radiography technique that warrants further investigation in the assessment of diaphragm dysfunction](https://bit.ly/3HFriWk)
<https://bit.ly/3HFriWk>

Cite this article as: FitzMaurice TS, McCann C, Nazareth DS, *et al.* Characterisation of hemidiaphragm dysfunction using dynamic chest radiography: a pilot study. *ERJ Open Res* 2022; 8: 00343-2021 [DOI: 10.1183/23120541.00343-2021].

Copyright ©The authors 2022

This version is distributed under the terms of the Creative Commons Attribution Non-Commercial Licence 4.0. For commercial reproduction rights and permissions contact permissions@ersnet.org

Received: 20 May 2021
Accepted: 12 Nov 2021

Abstract

Objectives Dynamic chest radiography (DCR) is a novel real-time digital fluoroscopic imaging system that produces clear, wide field-of-view diagnostic images of the thorax and diaphragm in motion, alongside novel metrics on moving structures within the thoracic cavity. We describe the use of DCR in the measurement of diaphragm motion in a pilot series of cases of suspected diaphragm dysfunction.

Methods We studied 21 patients referred for assessment of diaphragm function due to suspicious clinical symptoms or imaging (breathlessness, orthopnoea, reduced exercise tolerance and/or an elevated hemidiaphragm on plain chest radiograph). All underwent DCR with voluntary sniff manoeuvres.

Results Paradoxical motion on sniffing was observed in 14 patients, and confirmed in six who also underwent fluoroscopy or ultrasound. In four patients, DCR showed reduced hemidiaphragm excursion, but no paradoxical motion; in three, normal bilateral diaphragm motion was demonstrated. DCR was quick to perform, and well tolerated in all cases and with no adverse events reported. DCR was achieved in ~5 min per patient, with images available to view by the clinician immediately within the clinical setting.

Conclusion DCR is a rapid, well-tolerated and straightforward chest radiography technique that warrants further investigation in the assessment of diaphragm dysfunction.

Introduction

Dysfunction of the phrenic nerve can occur due to a range of disorders, including malignancy, trauma and neurological disease [1]. Phrenic nerve palsy and subsequent diaphragm paralysis is suggested by a malpositioned hemidiaphragm on plain chest radiograph or computed tomography (CT) scan, even though static images have low specificity for paralysis [2]. Coupled with a postural change in spirometry, real-time assessment looking for paradoxical motion is needed. Fluoroscopy, and more recently ultrasound, has been used for this visual confirmation of paradoxical motion; however, both techniques have important limitations in the diagnosis of hemidiaphragm paralysis [3].

A recent technological innovation is dynamic chest radiography (DCR), a low-dose cineradiographic imaging system in which sequential frames of the entire thorax are digitally reconstructed to produce a continuous moving image [4]. It occupies the same footprint as a standard chest radiography module and can also be used to provide plain radiographic imaging. DCR may carry advantages over traditional fluoroscopy in terms of ease of procedure and reduced radiation dose [5] and the production of quantitative data on diaphragm and chest wall motion [6, 7]; due to the ease of subject positioning and the digitised results produced, DCR may have the potential for less user-dependent measurement of diaphragm motion than ultrasound imaging.



DCR is licensed in the European Union, United States and Japan for cineradiographic thoracic imaging, and is in routine clinical use in our tertiary cardiothoracic centre for this purpose. DCR produces clear images of the diaphragm [7] (supplementary video) and has obvious potential for use in the assessment of moving structures in the thoracic cavity; here, we used it for the first time to assess diaphragm motion in a pilot series of cases of suspected phrenic nerve palsy.

Methods

Patients

With their consent, we studied 21 consecutive patients referred for assessment of diaphragm function at our tertiary cardiorespiratory centre: mean \pm SD age 61 \pm 13 years, n=7 female, height 172 \pm 10 cm, weight 90 \pm 15 kg, body mass index (BMI) 31 \pm 5 kg·m⁻²) based on suspicious plain chest radiograph findings (an abnormally postured hemidiaphragm), supportive clinical symptoms (breathlessness, orthopnoea, reduced exercise tolerance) and/or suggestive history (cardiac intervention, trauma, infection). Clinical characteristics and findings on plain radiography (CT, chest radiograph) are described in table 1.

Procedure

Patients were instructed to take three sharp sniffs followed by a breath to full inspiration then full expiration, with a trial run before exposure to ionising radiation in order to maximise compliance with breathing instructions. Instructions were read from a printed sheet by the performing radiographer. Images were acquired in the posteroanterior plane, in a standing position, with a maximum allowable image exposure time of 300 frames, or 20 s. Time taken for preparation, patient instruction and image acquisition was ~5 min per patient, broadly comparable to the time needed to perform a standard chest radiograph. Details of the equipment and technique used are available in the supplementary material.

Image analysis

The proprietary software did not allow for automated diagnosis, so DCR images were reviewed independently by a thoracic radiologist (CM) and a chest physician (TSF). Sniff tests were reported as positive if paradoxical (cranial) hemidiaphragm motion was observed during a sniff manoeuvre; reduced or absent caudal motion during sniff or deep breathing manoeuvres was noted. Automatic image analysis by proprietary software quantified peak hemidiaphragm speed (defined as the highest speed during inspiratory manoeuvres, determined by visual inspection of the diaphragm motion plot), excursion (maximum distance travelled by the diaphragm during inspiratory manoeuvre) and projected lung area (PLA), the visible area of lung as viewed in the posteroanterior projection). Sniff test positivity was made on visual inspection of DCR images alone; supplementary metrics calculated by the software were not necessary to confirm this. Statistics are presented as mean \pm SD, and the Wilcoxon signed-rank test is used for unpaired comparisons. Correlation is presented using the Pearson correlation coefficient.

Further tests

Spirometry was performed in the supine and erect postures in 18 patients; three also underwent diaphragm fluoroscopy and three also had diaphragm evaluation using ultrasound. Routinely collected demographic information was recorded from patient case notes.

Results

DCR was well tolerated by all patients and no adverse events were reported. Image acquisition took <20 s (mean 17 s), with ionising radiation mean estimated effective dose of 0.25 mSv. Results for cases of abnormal diaphragm motion are summarised in table 2; cases with no abnormal motion are summarised in table 3. Still DCR frames are shown in figure 1, and the speed/excursion graph produced by the DCR workstation for the same individual, available shortly after image capture, is shown in figure 2. A video of a dynamic chest radiograph in action is available in the supplementary material.

Visual inspection of DCR with spirometry and fluoroscopy

Of the 21 cases, 14 demonstrated paradoxical motion on sniffing during DCR, and in those who had undergone fluoroscopy or ultrasound (patients 3, 8, 11, 13, 18, 21), confirmed the results of the other imaging modality, to whose results the investigators were blinded. There were no disagreements between the first (CM) and second (TSF) observers. Four (patients 1, 5, 18, 20) showed reduced (that is, abnormal) hemidiaphragm excursion compared to the unaffected side, but no paradoxical motion. Three (patients 10, 14, 17) demonstrated normal bilateral hemidiaphragm motion with no parenchymal lung changes visible; none of these had demonstrated abnormally postured hemidiaphragms on preceding plain chest radiographs; rather, they had been referred for suggestive symptoms (breathlessness following cardiac procedures) only, and no subsequent diaphragmatic or parenchymal lung disease was diagnosed. In all three cases, symptoms resolved.

TABLE 1 Aetiology and plain imaging findings

Patient ID	Raised hemidiaphragm on chest radiograph	Further static imaging	Symptoms	Aetiology
1	Yes	CT thorax: ipsilateral lobectomy, no mass	Shortness of breath, cough	Post-thoracic surgery
2	Yes	CT thorax: no mass/other cause	Shortness of breath, reduced exercise tolerance	Infection
3	Yes	CT thorax: no mass/other cause	Shortness of breath, reduced exercise tolerance	Traumatic: neck hyperextension
4	Yes	CT thorax: no mass/other cause	Shortness of breath, reduced exercise tolerance	Idiopathic
5	Yes	CT thorax: no mass/other cause, right basal atelectasis (contralateral to abnormal diaphragm)	Shortness of breath, reduced exercise tolerance, cough, chest pain	Idiopathic
6	Yes	CT thorax: no mass/other cause, right basal atelectasis (contralateral to abnormal diaphragm)	Exertional breathlessness	Idiopathic
7	Yes	CT thorax: no mass; bronchiectasis and basal atelectasis bilaterally	Shortness of breath, reduced exercise tolerance	Idiopathic
8	Yes	CT thorax: no mass/other cause, healed rib fractures	Cough, shortness of breath	Traumatic: fall
9	Yes	CT thorax: no mass; atelectasis in upper and lower lobes bilaterally	Shortness of breath, reduced exercise tolerance	Idiopathic
10	No	CT thorax: no mass/other cause	Shortness of breath, cough	Normal
11	Yes	CT thorax: no mass/other cause	Shortness of breath	Idiopathic
12	Yes	CT thorax: no mass/other cause	Shortness of breath, reduced exercise tolerance	Phrenic nerve palsy of unknown aetiology
13	Yes	CT thorax: no mass/other cause, right basal atelectasis (contralateral to abnormal diaphragm)	Shortness of breath, reduced exercise tolerance	Idiopathic
14	No	CT thorax: no mass/other cause	Shortness of breath, fatigue	Normal
15	Yes	No CT	Shortness of breath	Idiopathic
16	Yes	CT thorax: LUL mass (contralateral to abnormal diaphragm)	Shortness of breath	Malignant
17	No	CT thorax: no mass/other cause	Shortness of breath	Normal
18	Yes	CT thorax: LLL consolidation (contralateral to abnormal diaphragm)	Shortness of breath, cough	Infection
19	Yes	CT thorax: no mass/other cause	Shortness of breath, cough	Idiopathic
20	Yes	CT thorax: pleural thickening, no mass	Shortness of breath, cough	Post-cardiac surgery
21	Yes	CT thorax: no mass/other cause	Shortness of breath	Idiopathic

CT: computed tomography; LUL: left upper lobe; LLL: left lower lobe.

TABLE 2 Findings on dynamic chest radiography sniff test: abnormal cases

Patient ID	Affected side	Inspiratory apex–diaphragm excursion [#] (mm)			Peak inspiratory apex–diaphragm speed [#] (mm·s ⁻¹)			Projected lung area change (%)			Standing/lying spirometry change (%)
		Normal	Abnormal	Difference	Normal	Abnormal	Difference	Normal	Abnormal	Difference	
1	Left [¶]	48	5	43	28	5	23	0.400	0.211	0.189	8.1
2	Left	40	-22	62	95	-31.5	126.5	0.280	0.293	-0.013	43.4
3	Right	29	-11	40	49	-25	74	0.297	0.229	0.068	5.6
4	Left	36	-36	72	77	-76	153	0.310	0.182	0.128	19.9
5	Left [¶]	48	15	33	49	21	28	0.348	0.240	0.108	2.5
6	Left	19	-15	34	54	-53	107	0.327	0.261	0.066	34.0
7	Left	32	-10	42	64	-11	75	0.361	0.145	0.216	5.4
8	Left	32	-6	38	62	-22	84	0.305	0.250	0.056	19.9
9	Left	25	-20	45	47	-31	78	0.223	0.083	0.140	15.4
11	Left	36	-19	55	72	-35	107	0.453	0.225	0.228	4.3
12	Right	19	-5	24	46	-18	64	0.182	0.305	-0.123	39.0
13	Left	31	-20	51	40	-24	64	0.149	0.118	0.031	34.2
15	Left	61	-24	85	51	-56	107	0.173	0.069	0.105	16.2
16	Right	22	-12	34	18.5	-30	48.5	0.232	0.057	0.174	5.2
18	Right [¶]	22.8	8.9	13.9	31	22	9	0.243	0.201	0.042	24.8
19	Right	32.8	-33.6	66.4	57.5	-9	66.5	0.239	0.122	0.117	7.7
20	Left [¶]	6.1	1.1	5	16.5	3	13.5	0.176	0.038	0.138	21.7
21	Left	9.4	-6.8	16.2	53.5	-17.5	71	0.298	0.168	0.130	20.0

[#]: a negative value denotes cranial motion; [¶]: reduced motion, but no paralysis demonstrated.

18 patients underwent erect and supine spirometry; in the 14 of these with paradoxical hemidiaphragm motion, there was a postural fall in forced vital capacity (FVC) of 19±13%. In two of the four cases in which DCR demonstrated reduced diaphragm excursion without paradoxical motion on sniff manoeuvre, two had nondiagnostic (*i.e.* <15%) change in FVC.

All but one patient underwent static CT imaging of the thorax. In all cases in which a raised hemidiaphragm had been seen on plain chest radiograph and dynamic chest radiography, this was confirmed on CT. In all cases in which ultrasound or fluoroscopy had also been carried out, DCR matched the findings.

Visual inspection of DCR and automatically calculated diaphragm motion

The hemidiaphragms are easily visible in the posteroanterior plane on DCR images and can be seen by both clinician and radiologist immediately without further image processing. In all cases, the observers' visual inspection of diaphragm motion on DCR matched that calculated by subsequently analysis of diaphragm motion using the DCR software. In the 14 patients with paradoxical diaphragm motion seen on DCR there was a significant difference in Δ PLA (the change in visible lung area between maximum inspiration and expiration) between the affected and unaffected sides (17.9±8.3% *versus* 27.4±8.1%, $p=0.002$). There was a significant difference in the magnitude of excursion (the absolute value, regardless of caudal/cranial direction of motion) during sniff manoeuvre between the affected and unaffected hemidiaphragms (15.0±9.7 *versus* 30.5±14.7 mm, $p=0.001$), and between the maximum speed during sniff manoeuvre between the affected and unaffected hemidiaphragm (27.2±18.7 *versus* 50.6±19.9 mm, $p<0.001$). Figure 3 demonstrates these associations. There was no significant difference in the magnitude

TABLE 3 Findings on dynamic chest radiography sniff test: normal cases

Patient ID	Inspiratory apex–diaphragm excursion (mm)			Peak inspiratory apex–diaphragm speed (mm·s ⁻¹)			Projected lung area change (%)		
	Right	Left	Difference	Right	Left	Difference	Right	Left	Difference
10	19	26	7	23	27	4	0.192	0.297	0.105
14	11.5	19.3	7.8	15	15	0	0.244	0.258	0.015
17	19.2	18.2	1	47.5	47.5	0	0.295	0.268	0.026

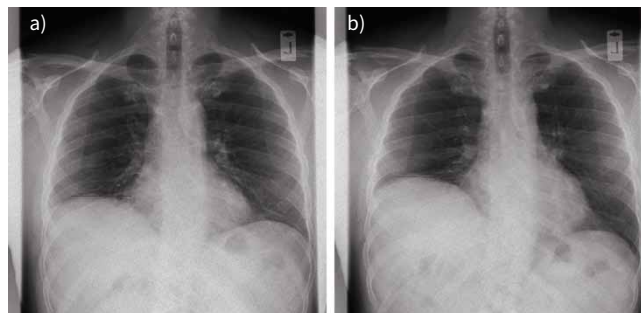


FIGURE 1 Two still images from a dynamic chest radiography (DCR) sequence showing paradoxical movement of the paralysed right hemidiaphragm from a) rest to b) end sniff manoeuvre.

of difference between the affected/unaffected sides when comparing affected left *versus* affected right hemidiaphragm speed, excursion or Δ PLA. There was a moderate but insignificant difference between the unaffected left and unaffected right hemidiaphragm excursion (32.6 ± 15.4 *versus* 25.1 ± 5.6 mm, $p=0.217$), and between the unaffected right and unaffected left hemidiaphragm speed during sniff manoeuvre (54.5 ± 20.5 *versus* 40.4 ± 15.5 mm, $p=0.183$). There was a significant correlation between maximum inspiratory hemidiaphragm speed (unaffected side) and BMI ($R^2=0.31$, $p=0.019$) (figure 3).

Discussion

DCR is a rapid, well-tolerated and new technique to assess diaphragm motion. In a short period of time it produces clear, visually obvious images of the diaphragm in motion. Unlike the smaller images of

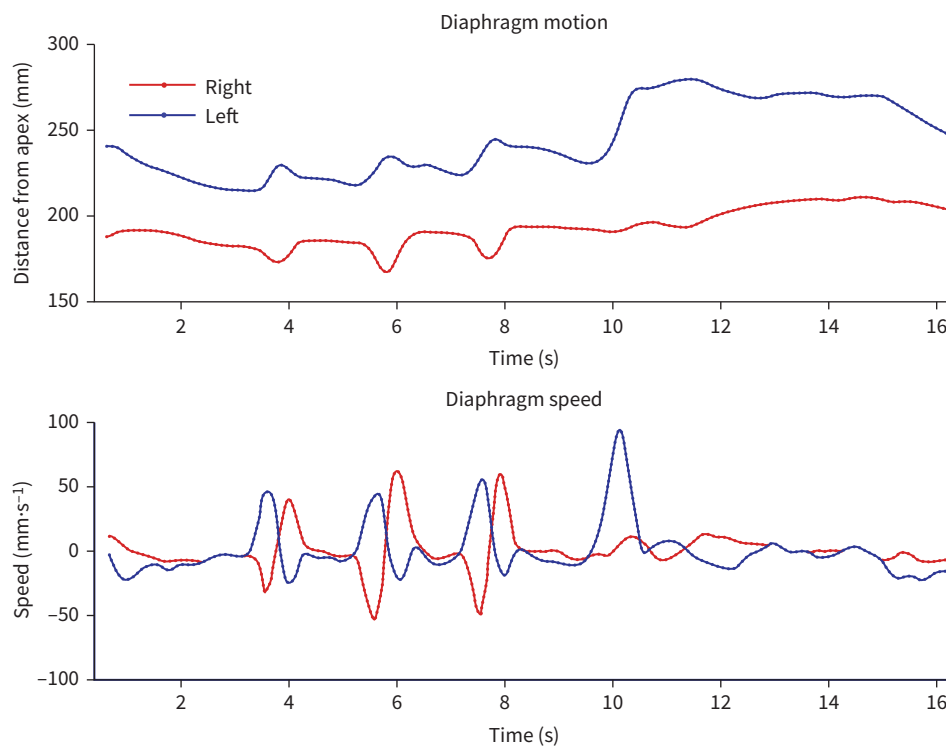


FIGURE 2 Diaphragm excursion and speed throughout the manoeuvre. Note the paradoxical motion of the paralysed right hemidiaphragm during three sniffs with corresponding negative acceleration and delayed rebound, and lack of motion during the subsequent deep inspiratory manoeuvre. These graphs are automatically generated and available after image capture for review by the clinician. Axis labels have been enlarged and simplified for clarity.

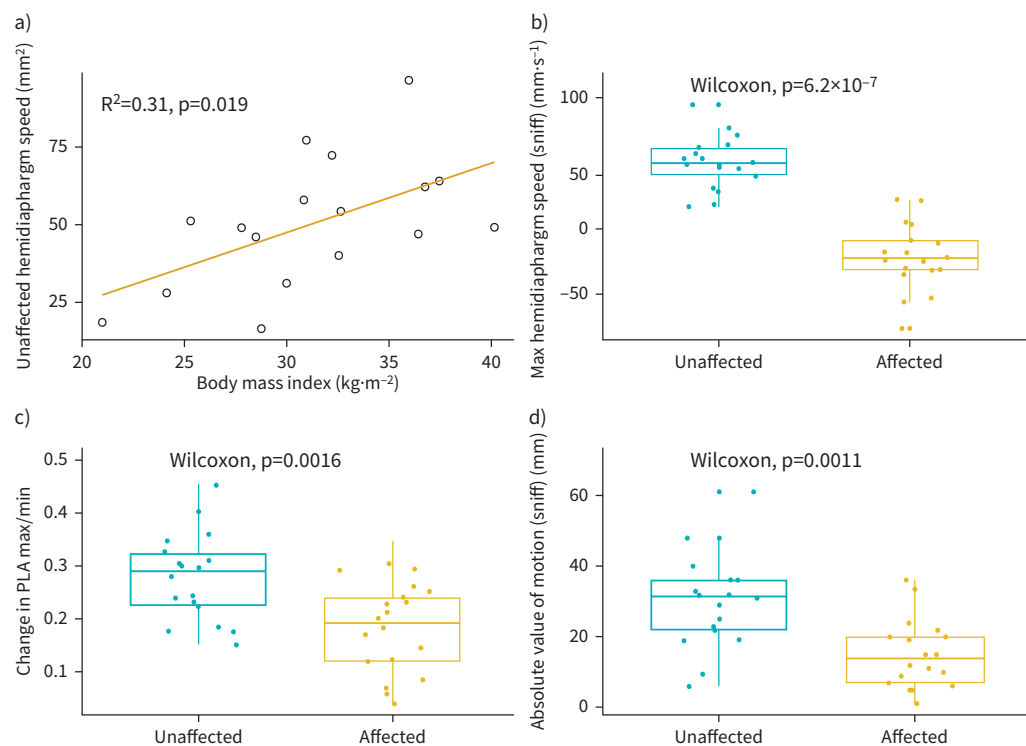


FIGURE 3 Data generated from dynamic chest radiography images. **a)** Correlation between unaffected hemidiaphragm speed and body mass index; **b)** difference in maximum hemidiaphragm speed; **c)** change in projected lung area (PLA) between maximum inspiration and expiration; **d)** absolute distance of hemidiaphragm excursion.

fluoroscopy, it has a wide, high-resolution field of view that encompasses the entire thoracic cavity, allowing concurrent diagnostic imaging and obviating the need for a supplementary chest radiograph. Clear differences in diaphragm motion are demonstrated between healthy and abnormal hemidiaphragms using DCR that were consistent with the appearances visualised by the reporting radiographer. DCR produces novel metrics on diaphragm and chest wall motion, which may be of further research interest. In those cases in which ultrasound or fluoroscopy had also been carried out, DCR matched the sniff test findings.

Due to the limited cases where concurrent comparator techniques were carried out (three cases with traditional fluoroscopy and three with ultrasound), this work cannot reliably comment on the specificity of DCR in the diagnosis of diaphragm paralysis, but may hold several potential advantages over traditional fluoroscopy and ultrasound in the assessment of diaphragm dysfunction. Furthermore, although chest wall and abdominal musculature can influence diaphragm motion by altering intrathoracic pressure, such changes will not be unilateral and therefore paradoxical motion of one hemidiaphragm, especially during a forced respiratory manoeuvre, is suggestive of its denervation. We postulate that the significant difference in speed during sniff manoeuvre between the afflicted and unaffected hemidiaphragms seen here represent a reduction in muscle strength on the afflicted side.

Traditionally, fluoroscopy is used to visualise the diaphragm during respiration: it is relatively quick to perform and is easily interpretable. However, it requires radiologist supervision, a dedicated fluoroscopy system, and may confer a significant radiation dose (upwards of 0.3 mSv): in order to reduce exposure, the field of view is necessarily small, excluding much of the lung parenchyma visible on a plain chest radiograph. Furthermore, the images acquired are not digitised, limiting their value.

M-mode ultrasound is portable and utilises a voluntary sniff test to provide results without ionising radiation, as well as measuring diaphragm thickness and thickening ratio. However, it requires skill and regular practice; this necessary expertise may not be readily available in some units. The values generated automatically by DCR might in future address the problems of reproducibility seen in ultrasound [8]. Whereas visualisation of the diaphragm by ultrasound may be obscured by the descending hemidiaphragm,

this is also not the case with DCR. DCR has a much shorter acquisition time than ultrasound or fluoroscopy, with visual results available to the ordering clinician immediately after acquisition, at a lower radiation dose than fluoroscopy. Dynamic magnetic resonance imaging (MRI) has been employed as a tool to analyse diaphragm function [9, 10], but is not in routine clinical use due to its high cost and limited availability. The small footprint of DCR allows installation in a standard radiography room, rather than a separate fluoroscopy or MRI suite.

This pilot work has some limitations. Only six cases were compared against an established reference technique of diaphragm motion assessment such as ultrasound or fluoroscopy, and no cases made comparison to phrenic nerve stimulation studies or phrenic nerve electromyography. There is a lack of normative data in the form of healthy comparators, which may be a focus for future studies in this area.

DCR has been used to assess average diaphragm excursion during tidal and deep breathing in healthy volunteers [7, 11], and abnormal diaphragm dynamics in people with severe COPD [12], and pulmonary perfusion [13, 14]. Similar correlations between BMI and diaphragm motion, as shown in this work, have been demonstrated by HATA *et al.* [5] in healthy volunteers.

To our knowledge, this is the first time DCR has been used in the investigation of hemidiaphragm dysfunction, and there remains large potential for further work in characterisation of the abnormal diaphragm, for example following surgical plication. No single imaging or spirometric technique can accurately diagnose diaphragm paralysis, and each has its own advantages and disadvantages [3]. DCR, which combines the visual ease of fluoroscopy with the ability to provide quantifiable measures of hemidiaphragm and chest wall movement, may be of use as an adjunct technique. These metrics may also be of use in disease monitoring and outcome prediction, for example after thoracic surgery and other scenarios where forced respiratory manoeuvres for lung volume measurement are problematic. However, the effort-dependent nature of any voluntary technique to assess diaphragm motion [3] may still prove problematic. Here, DCR proved quick and straightforward to perform. It produces easily interpretable metrics on diaphragm and chest wall motion that warrant further study alongside established diagnostic tools such as ultrasound and traditional fluoroscopy. Larger studies are warranted based on these initial results.

Acknowledgements: The authors would like thank the radiographers Rachel Diamond, Stephen Lomax and Nicola Hepplestone-Downes (Dept of Radiology, Liverpool Heart and Chest Hospital, Liverpool, UK), for their efforts coordinating and acquiring the dynamic chest radiographs used in this work. We are grateful to the patients included in this work, on whose images it is based.

Provenance: Submitted article, peer reviewed.

Conflict of interest: None declared.

References

- 1 Laghi F, Tobin MJ. Disorders of the respiratory muscles. *Am J Respir Crit Care Med* 2003; 168: 10–48.
- 2 Chetta A, Rehman AK, Moxham J, *et al.* Chest radiography cannot predict diaphragm function. *Respir Med* 2005; 99: 39–44.
- 3 Laghi FA, Saad M, Shaikh H. Ultrasound and non-ultrasound imaging techniques in the assessment of diaphragmatic dysfunction. *BMC Pulm Med* 2021; 21: 85.
- 4 Tanaka R, Sanada S, Okazaki N, *et al.* Evaluation of pulmonary function using breathing chest radiography with a dynamic flat panel detector: primary results in pulmonary diseases. *Invest Radiol* 2006; 41: 735–745.
- 5 Hata A, Yamada Y, Tanaka R, *et al.* Dynamic chest X-ray using a flat-panel detector system: technique and applications. *Korean J Radiol* 2021; 22: 634–651.
- 6 Hino T, Hata A, Hida T, *et al.* Projected lung areas using dynamic X-ray (DXR). *Eur J Radiol Open* 2020; 7: 100263.
- 7 Hida T, Yamada Y, Ueyama M, *et al.* Time-resolved quantitative evaluation of diaphragmatic motion during forced breathing in a health screening cohort in a standing position: dynamic chest phrenicography. *Eur J Radiol* 2019; 113: 59–65.
- 8 Boussuges A, Gole Y, Blanc P. Diaphragmatic motion studied by M-mode ultrasonography: methods, reproducibility, and normal values. *Chest* 2009; 135: 391–400.
- 9 Unal O, Arslan H, Uzun K, *et al.* Evaluation of diaphragmatic movement with MR fluoroscopy in chronic obstructive pulmonary disease. *Clin Imaging* 2000; 24: 347–350.

- 10 Le Pimpec-Barthes F, Hernigou A, Mazzella A, *et al.* Dynamic magnetic resonance imaging in unilateral diaphragm eventration: knowledge improvement before and after plication. *J Thorac Dis* 2019; 11: 3467–3475.
- 11 Yamada Y, Ueyama M, Abe T, *et al.* Time-resolved quantitative analysis of the diaphragms during tidal breathing in a standing position using dynamic chest radiography with a flat panel detector system (“dynamic X-ray phrenicography”): initial experience in 172 volunteers. *Acad Radiol* 2017; 24: 393–400.
- 12 Hida T, Yamada Y, Ueyama M, *et al.* Decreased and slower diaphragmatic motion during forced breathing in severe COPD patients: time-resolved quantitative analysis using dynamic chest radiography with a flat panel detector system. *Eur J Radiol* 2019; 112: 28–36.
- 13 Yamamoto S, Hasebe T, Tomita K, *et al.* Pulmonary perfusion by chest digital dynamic radiography: comparison between breath-holding and deep-breathing acquisition. *J Appl Clin Med Phys* 2020; 21: 247–255.
- 14 Tanaka R, Tani T, Nitta N, *et al.* Detection of pulmonary embolism based on reduced changes in radiographic lung density during cardiac beating using dynamic flat-panel detector: an animal-based study. *Acad Radiol* 2019; 26: 1301–1308.